Int. j. inf. tecnol.
https://doi.org/10.1007/s41870-024-01791-4

ORIGINAL RESEARCH

Improvisation of artificial hummingbird algorithm through incorporation of chaos theory in intelligent optimization of fractional order PID controller tuning

Hrishikesh Sarma[1] · **Aroop Bardalai**[1]

Received: 10 November 2023 / Accepted: 13 February 2024

Abstract Artificial hummingbird algorithm (AHA) is one of the recent bio-inspired meta-heuristic algorithms which is based on hummingbirds' intelligent behaviours. Just like many meta-heuristic algorithms, it also suffers from freezing in local optima and slow convergence speed. In this paper, the authors have proposed a novel chaotic artificial hummingbird algorithm (ChAHA) obtained by incorporating chaos theory in the original AHA with the aim of escaping it from local minima stagnation along with high convergence rate and more precise results. Firstly, detailed studies have been performed on six different unimodal and multimodal constrained benchmark functions by employing ten different chaotic test mappings in order to determine the most enhanced and efficient one. Later, statistical testing and graphical analysis prove that incorporation of chaotic maps (especially tent map) in AHA improves the original AHA by showing promising performance. Finally, the performance of the ChAHA (with tent map) is also validated by finding the optimum gain values of a fractional order proportional-integral-derivative (FOPID) controller, meticulously tailored to meet the specific requirements of DC motor speed control in MATLAB/Simulink. It has been unambiguously affirmed that the closed loop system with the proposed ChAHA-FOPID controller has better performance than certain pre-existing controllers such as grey wolf optimization based FOPID (GWO-FOPID), atom search optimization based FOPID (ASO-FOPID) and manta ray foraging optimization based FOPID (MRFO-FOPID) controllers. Finally, robustness analysis is also carried out with parameter variations of DC motor and the final simulation results validate the superiority of the proposed approach.

Keywords Chaotic map · Artificial hummingbird algorithm · DC motor · Fractional order PID controller · ITAE objective function · Robustness analysis

1 Introduction

In computational intelligence, the aim of optimization is to find the optimal or near-optimal solutions to a given issue within a predetermined search space. The urge to address complex and non-linear optimization issues has led to constant evolution of algorithmic approaches. Though classical optimization techniques are fruitful in limited situations, they fail to overcome insurmountable barriers while addressing high-dimensional, complex and non-linear problem environments [1]. Many researchers have been attracted towards metaheuristic algorithms owing to their special ability to penetrate through solution spaces efficiently in the process of solving such intricate problems. Getting inspired from social and natural phenomena, these algorithms have a built-in capacity to thoroughly explore and exploit the search space in an attempt to discover the global optima in reasonable time-period.

One of the research domains with the most rapid development is meta-heuristic optimization approaches. Credit belongs to the No Free Lunch (NFL) theorem, which proclaims that there isn't an ideal algorithm that can resolve every problem better than any other method [2]. This encouraged the authors of this paper to come up with a novel meta-heuristic method through improving an existing

✉ Hrishikesh Sarma
hrishikeshsarma2012@gmail.com

Aroop Bardalai
abardalai.ele@aec.ac.in

[1] Department of Electrical Engineering, Assam Engineering College, Guwahati, Assam, India

Published online: 27 March 2024

one. A typical shortcoming of most meta-heuristics is their inability to dynamically change user-defined parameters, and diverse control parameter selections have varying impacts on optimization results [3]. Moreover, many optimizers have several control parameters. Consequently, it is imperative to examine the trend of parameter influence on the entire algorithm, as this will unavoidably lead to an increase in needless computation and operating expenses. Furthermore, a lot of optimizers consist of several control parameters. Selecting different parameters to solve various optimization problems proves to be difficult. Because of this, an algorithm with fewer control parameters must be designed.

An algorithm meeting the above criteria is artificial hummingbird algorithm (AHA), a very recent bio-inspired optimization algorithm that draws inspiration from the intelligent behaviour of hummingbird [4]. It mimics the hummingbird's unique flight abilities and foraging techniques which includes axial, diagonal and omnidirectional flights. It has been established that this algorithm produces better results than other meta-heuristic algorithms in real world scenarios [5–8]. However, similar to majority of meta-heuristic algorithms, the basic problem with AHA is its slow search performance, poor optimization precision, and premature convergence leading to researchers for developing its improved versions [9–16]. Table 1 lists some of the relevant works based on AHA and its modified version with different approaches. Wang et al. [9] introduced the golden sine factor in the AHA to solve truss topology engineering problem considering both static and dynamic constraints. Ramadan et al. [10] employed an opposition-based learning method for improving AHA and is experimented on static and dynamic models of photovoltaic solar cell to prove its efficacy over supply-demand-based optimization (SDO), wild horse optimizer (WHO), and tunicate swarm algorithm (TSA). Ali et al. [11] proposed two improved AHA versions, random opposition-based learning (ROBL) and opposition-based learning (OBL), in tackling waste classification problem based on relevant feature selection along with a comparative analysis among twelve advanced optimizers. Aquila optimization (AO) is hybridized with AHA by Elaziz et al. [12] for effective feature selection from four different raw medical image datasets. Sarhana et al. [13] proposed an enhanced artificial hummingbird optimizer (EAHO) by integrating linear control mechanism (LCM) and diverse territorial foraging strategies (TFSs) into the traditional AHA for optimizing power flow in IEEE 30, 57, and 118-bus test grids. Yildiz et al. [14] presented in a hybrid model of AHA and simulated annealing (AHA-SA) and had used to solve complex multi-constrained optimization problems prevalent in mechanical engineering domains. In Emam et al. [15], local escape operator (LEO) and OBL are integrated together in basic AHA resulting in a modified AHA (mAHA). This is then applied in modified IEEE-30 bus and IEEE-118 bus systems for solving real-world OPF problem in addition to performance comparison with whale optimization algorithm (WOA), sine cosine algorithm (SCA), TSA, slime mould algorithm (SMA), harris hawks algorithm (HHA), RUNge kutta optimization algorithm (RUN), and basic AHA. AHA is amalgamated with genetic operators to generate mAHA by Alhumade et al. [16] for solving maximum power point tracking (MPPT) on a single sensor-based photovoltaic systems.

Literature has shown us that chaos theory is a strong contender for improving the efficacy of meta-heuristic methods

Table 1 Some significant works on AHA

Approach	Areas of application	References
AHA	RDGs planning optimization under uncertainties	[5]
AHA	Parameter estimation of solar modules	[6]
AHA	Energy management of microgrids with demand response	[7]
AHA	Optimization of biomass-based DGs in radial distribution network	[8]
Golden sine factor based enhanced AHA (DGSAHA)	Optimization of truss topology in engineering	[9]
Adaptive opposition AHA (AOAHA)	Accurate static and dynamic photovoltaic models	[10]
Improved AHA using random opposition-based learning (AHA-ROBL)	Feature selection-based waste classification problem	[11]
Hybrid AHA with aquila optimization (AHA-AO)	Optimal feature selection in medical image classifier	[12]
AHA with linear control mechanism (LCM) and diverse territorial foraging strategies (TFSs)	Power flow optimization in IEEE 30, 57, and 118-bus test grids	[13]
Hybrid AHA with simulated annealing (AHA-SA)	Constrained mechanical engineering issues	[14]
AHA with local escape operator (LEO) and OBL	Optimal power flow (OPF) problem in modified IEEE-30 bus and IEEE-118 bus systems	[15]
AHA with genetic operators	Maximum power point tracking (MPPT) optimization for photovoltaic (PV) cells	[16]

and has been extensively applied in many applications since the advent of nonlinear dynamics. The incorporation of chaos theory with optimization techniques is one of the most well-known applications in this domain [17–19]. Literature reveals that several meta-heuristic optimization techniques have so far been effectively paired with chaos theory [20–32]. Kohli and Arora [20] introduced ten different chaotic maps in grey wolf optimization (GWO) algorithm in an attempt to accelerate its convergence rate and is analyzed on thirteen constrained benchmark functions. Chebyshev map is found out to be the most efficient map and the proposed approach is validated on five constrained engineering problems. Ahmad et al. [21] introduced chaotic particle swarm optimization (PSO) in the area of image encryption where logistic map helps in initial population generation followed by PSO in achieving optimization of encryption process. Misaghi and Yaghoobi [22] proposed and investigated chaotic invasive weed optimization (IWO) algorithm on five benchmark functions. The authors have used logistic chaotic map for determining the optimal gain values of a PID controller for a DC motor speed control. Arora and Anand [23] have successfully improved the global convergence rate of grasshopper optimization algorithm (GOA) through the utilization of chaotic map functions with circle map proving to be the most efficient one. Hybridization of salp swarm algorithm (SSA) with chaos theory was proposed by Sayed et al. [24]. SSA with ten chaotic maps are applied on fourteen benchmark problems and twenty benchmark datasets resulting in logistic chaotic map as the efficient one. In Kaur and Arora [25], the performance of WOA is improved by employing ten chaotic maps (especially tent map) with an enhanced speed of convergence. Twenty benchmark functions have been used for qualitative analysis and statistical testing of this proposed technique. Arora and Singh [26] examined the functionality of ten varied chaotic maps in enhancing butterfly optimization algorithm (BOA). Also, the proposed approach is employed on certain test functions for proper validation along with solving engineering design problems. With the goal of enhancing biogeography-based optimization (BBO), Saremi et al. [27] utilized ten chaotic maps for defining certain probabilistic parameters. Performance evaluation is done on ten test functions and the result showed that gauss map can significantly enhance the original algorithm. Verma et al. [28] has proposed chaotic Archimedes optimization algorithm (AOA) as an improved version of the original algorithm which is further employed in solving Regression test selection issue. Statistical testing proved singer map to be the most effective chaotic map among ten selective chaotic maps. Shinde et al. [29] presented modified enhanced version of SCA with the help of ten chaotic maps and comparative analysis of the work was done on nineteen benchmark functions along with other advanced algorithms besides solving four engineering problems. Bansal and Sahoo [30] introduced chaos dynamics into gorilla troops optimizer (GTO) for improving its global search capability. This is further employed in non-negative matrix factorization (NMF) problem for successful integrative analysis of four varied cancer data source. Alam and Muqeem [31] have proposed chaos game optimization (CGO) based Recurrent Neural Network (RNN) for prediction of heart disease with greater efficiency and accuracy. Mirjalili and Gandomi [32] suggested a chaotic version of gravitational search algorithm (GSA) employing ten chaotic maps for proper balancing exploration and exploitation phases. Evaluation of the proposed approach was performed on twelve benchmark functions and upon statistical testing sinusoidal map came out to be the best map in performance improvement of GSA.

With the goal of accelerating AHA's rate of convergence, the authors of the present work have proposed a novel hybridization methodology based on AHA and chaos theory. It has been demonstrated in the literature that substituting chaotic systems for random numbers in mathematical models enhances the algorithm's capacity for global convergence and avoids local optimum stagnation [33]. As a result, the major parameters of AHA are replaced with ten different one-dimensional chaotic maps in order to completely assess the efficaciousness of chaos theory for boosting its exploration and/or exploitation capabilities. Six benchmark unimodal and multimodal functions are chosen to estimate the performance of the proposed method. The findings of the simulations demonstrate that the chaotic artificial hummingbird algorithm (ChAHA) outperforms the original AHA in context of proficiency and precision. For emphasizing the persuasiveness of the proposed ChAHA, the authors have implemented it to conduct meticulous optimum tuning of a Fractional Order Proportional-Integral-Derivative (FOPID) controller for accomplishing precise DC motor speed control. FOPID controller have additional fractional order parameters in addition to traditional proportional-integral-derivative (PID) parameters. This expanded parameter space leads to increased system complexity and the tuning process more intricate [34]. As such, tuning of a FOPID controller for DC motor speed control remains to be a matter of great concern for the control engineers as the system performance greatly depends on the optimal values of its five functioning parameters. Heuristic optimization techniques are often tested in real-world scenarios through the tuning of controller parameters for DC motor speed regulation. Some of the recent notable metaheuristic optimization methods used to tune FOPID controllers so as to obtain DC motor speed control as found in literature works are gazelle optimization algorithm (GOA) [35], improved slime mould algorithm (SMA) [36], GWO [37], atom search optimization (ASO) [38], and manta ray foraging optimization (MRFO) [39]. Furthermore, the authors have

not found any existing literature where a FOPID controller has been tuned using artificial hummingbird algorithm (AHA), thereby making it a novel approach.

In this work, the authors have selected integral of time multiplied absolute error (ITAE) as the objective function which needs to be minimized in order to accomplish the controller tuning. An honest comparison of the suggested ChAHA-FOPID and AHA-FOPID controllers are performed with some of the pre-existing approaches in literature such as GWO-FOPID [37], ASO-FOPID [38], and MRFO-FOPID [39] controllers. Additionally, the proposed controller's robustness analysis is performed when the DC motor configurations are varied, and the findings are shown in both graphical and tabular formats for easier comprehension.

The major contributions and novelties of this paper are listed as follows:

(i) A novel chaotic version of AHA obtained by incorporation of chaos theory into AHA is proposed for accelerating the convergence rate of AHA.
(ii) Ten different chaotic maps are used and the proposed chaotic version of AHA (i.e. ChAHA) is applied on six constrained benchmark functions and their detailed performance evaluations are carried out along with statistical testing and graphical analysis.
(iii) Both the proposed ChAHA and the original AHA techniques are employed for the first time in motor drive application area of electrical engineering field in performing efficient tuning of a FOPID controller in DC motor speed control.
(iv) Comparative analysis of the proposed approaches with certain pre-existing cutting-edge controller types such as GWO-FOPID [37], ASO-FOPID [38], and MRFO-FOPID [39] are performed in terms of time domain transient response analysis by minimization of same ITAE objective function.
(v) Robustness analysis of the proposed ChAHA approach under sudden variations of DC motor parameter variations are done and are also compared with the other pre-existing approaches.

The remaining of the paper is arranged as follows: Sect. 2 contains briefly an overview of the conventional AHA. Section 3 describes the chaotic maps that depict chaotic sequences for AHA. The proposed ChAHA is presented in Sect. 4. Performance evaluations in terms of statistical testing and graphical analysis of proposed ChAHA are described in Sect. 5. This is followed by Sect. 6 consisting of mathematical model of both DC motor and FOPID controller. Design and implementation of ChAHA-FOPID controller for controlling the speed of DC motor is presented in Sect. 7. Section 8 includes comparative analysis with some of the pre-existing controller approaches while Sect. 9 contains the robustness analysis. Finally, conclusion in Sect. 10 marks the end of the paper.

2 Artificial hummingbird algorithm (AHA)

AHA is a newly developed bio-inspired meta-heuristic optimization algorithm, basically getting inspired from the astute feeding behaviour of hummingbirds [4]. The AHA algorithm involves three main steps: exploration, exploitation, and updating and is mathematically presented as follows.

2.1 Initialization

The algorithm starts with a population of m hummingbirds placed on m sources of food which gets randomly initialized by Eq. (1).

$$y_a = lb + r_1 \cdot (ub - lb);\ a = 1, \ldots, m \tag{1}$$

where, lb and ub represents respective lower and upper limits for a specific issue, r_1 is a vector of random values within [0, 1], and y_a denotes the ath source of food position marking the specified issue solution.

The visit table of food sources is created as in Eq. (2).

$$VT_{a,b} = \begin{cases} 0; & a \neq b;\ a = 1, \ldots, m;\ b = 1, \ldots, m \\ null; & a = b \end{cases} \tag{2}$$

where, the first condition states that the ath hummingbird has just visited the bth source of food while the second condition says that a hummingbird is feeding at its designated source of food.

2.2 Guided foraging

This algorithm uses a direction switch vector to control and supervise omnidirectional, diagonal and axial flight directions of hummingbirds during foraging in the s-dimension space.

The above-mentioned flight sequences can be expanded to a s-S space, with Eq. (3) defining the axial flight ability.

$$S^a = \begin{cases} 1; & a = randa([1, s]);\ a = 1, \ldots, s \\ 0; & else \end{cases} \tag{3}$$

Equation (4) defines the diagonal flight ability while Eq. (5) is for omnidirectional flight ability.

$$S^a = \begin{cases} 1; & a = P(b);\ b \in [1, f];\ P = randperm(f);\ for\ f \in [2, \lceil r_2(s-2) \rceil + 1] \\ 0; & else \end{cases} \tag{4}$$

$$S^a = 1; a = 1, \ldots, s \tag{5}$$

where, *randa*([1, s]) creates an arbitrary integer between 1 to *s*, *randperm*(*f*) generates an arbitrary permutation of integers between 1 to *f*, and r_2 is any arbitrary number within [0, 1].

Guided foraging behaviour and a potential source of food are represented mathematically as in Eqs. (6) and (7) respectively.

$$u_a(t+1) = y_{a,tgt}(t) + GF \cdot S \cdot (y_a(t) - y_{a,tgt}(t)) \tag{6}$$

$$GF \sim N(0, 1) \tag{7}$$

where $y_a(t)$ denotes the ath source of food position at t time, $y_{a,tgt}(t)$ denotes position of the intended source of food, GF denotes guided factor, and $N(0, 1)$ is the normal distribution with a mean of 0 and standard deviation of 1.

As per Eq. (8), the ath source of food position gets updated.

$$y_a(t+1) = \begin{cases} y_a(t); & f(y_a(t)) \le f(u_a(t+1)) \\ u_a(t+1); & f(y_a(t)) > f(u_a(t+1)) \end{cases} \tag{8}$$

where $f(\bullet)$ represents value of fitness function.

2.3 Territorial foraging

In territorial foraging strategy, Eq. (9) can be useful in tracing of hummingbirds locally while a candidate source of food is obtained mathematically as in Eq. (10).

$$u_a(t+1) = y_a(t) + TF \cdot S \cdot y_a(t) \tag{9}$$

$$TF \sim N(0, 1) \tag{10}$$

where TF denotes territorial factor and $N(0, 1)$ is the normal distribution with a mean of 0 and standard deviation of 1.

2.4 Migration foraging

A hummingbird with the lowest rate of nectar refilling migrates to hunt randomly from the previous source to a new one, as given by Eq. (11).

$$y_{wst}(t+1) = lb + r_3 \cdot (ub - lb) \tag{11}$$

where, y_{wst} represents source of food with the lowest nectar refiling rate, and r_3 is a random vector within [0, 1]. The algorithm suggests Eq. (12) as a desirable definition for the migration coefficient (MC) in terms of population size (m).

$$MC = 2m \tag{12}$$

3 Chaotic maps

In any dynamic non-linear system characterized by non-repetitive, non-converging, and constrained, chaos is a randomized deterministic method which replaces random variables by chaotic variables. As a result, it can execute more faster search operation than probabilistic or stochastic search. In the realm of optimization, a broad range of unique chaotic maps are available [40]. In the current work, the ten most popular unidimensional chaotic maps have been used [22–29]. Table 2 provides an overview of the mathematical variations of these chaotic maps where, k stands for index count corresponding to chaotic series x; x_k represents the chaotic series of the kth number; a and b denotes the controlling parameters, influencing the dynamic system's chaotic nature. All the chaotic maps are initialized from the same starting point $x_0 = 0.7$, the reason being that the initial value greatly influences the fluctuation patterns on chaotic maps [27]. Figure 1 shows the visualization of chaotic maps for 100 number of iterations.

4 The proposed novel chaotic artificial hummingbird algorithm (ChAHA)

In this section, a novel chaotic artificial hummingbird algorithm (ChAHA) is proposed wherein chaotic maps are employed to replace the three random variables r_1, r_2 and r_3 with chaotic variables. The original algorithm has three main parameters r_1, r_2 and r_3 which affect its performance. Parameter r_1 is responsible for random initialization of the solutions as given in Eq. (1), r_2 refers to guided foraging strategy (exploration as well as exploitation) as given in Eq. (4), while r_3 refers to migration foraging strategy (exploration) as given in Eq. (11). During guided foraging, r_2 controls the direction switch vector which in turn manages the three special flight skills for the speedy merging of hummingbirds approaching the destination updating repeatedly throughout the course of iterations as can be seen in Eq. (4). According to Eq. (6), exploration is prioritized initially due to significant distance between food sources, but progressively as the distance reduces, exploitation is prioritized. Thus, r_2 significantly impact on balancing between exploration and exploitation. In this study, the authors have used the chaotic map to adjust the r_2 parameter of AHA and is named as the ChAHA which is shown in Eq. (13). An illustration of the flowchart of proposed ChAHA algorithm is presented in Fig. 2.

$$S^a = \begin{cases} 1; \ a = P(b); b \in [1, f]; P = randperm(f); f \in [2, \lceil r_2(t) \cdot (s-2) \rceil + 1] \\ 0; \ else \end{cases} \tag{13}$$

Table 2 Chaotic maps [22–29]

No.	Name	Chaotic map equations
ChAHA1	Chebyshev	$x_{k+1} = \cos(k\cos^{-1}(x_k))$
ChAHA2	Circle	$x_{k+1} = x_k + b - \left(\frac{a}{2\pi}\right)\sin\left(2\pi x_k\right) mod(1);\ a = 0.5,\ b = 0.2$
ChAHA3	Gauss/mouse	$x_{k+1} = \begin{cases} 0; & x_k = 0 \\ \frac{1}{x_k mod(1)}; & otherwise \end{cases}$ $\frac{1}{x_k mod(1)} = \frac{1}{x_k} - \left[\frac{1}{x_k}\right]$
ChAHA4	Iterative	$x_{k+1} = \sin\left(\frac{a\pi}{x_k}\right);\ a = 0.7$
ChAHA5	Logistic	$x_{k+1} = a x_k\left(1 - x_k\right);\ a = 4$
ChAHA6	Piecewise	$x_{k+1} = \begin{cases} \frac{x_k}{a}; & 0 \le x_k \le a \\ \frac{x_k - a}{0.5 - a}; & a \le x_k \le 0.5 \\ \frac{1 - a - x_k}{0.5 - a}; & 0.5 \le x_k \le (1 - a) \\ \frac{1 - x_k}{a}; & (1 - a) \le x_k \le 1 \end{cases};\ a = 0.4$
ChAHA7	Sine	$x_{k+1} = \frac{a}{4}\sin\left(\pi x_k\right);\ a = 4$
ChAHA8	Singer	$x_{k+1} = a\left(7.86x_k - 23.31x_k^2 + 28.75x_k^3 - 13.302875x_k^4\right);\ a = 1.07$
ChAHA9	Sinusoidal	$x_{k+1} = a x_k^2 \sin\left(\pi x_k\right);\ a = 2.3$
ChAHA10	Tent	$x_{k+1} = \begin{cases} \frac{x_k}{0.7}; & x_k < 0.7 \\ \frac{10}{3}\left(1 - x_k\right); & x_k \ge 0.7 \end{cases}$

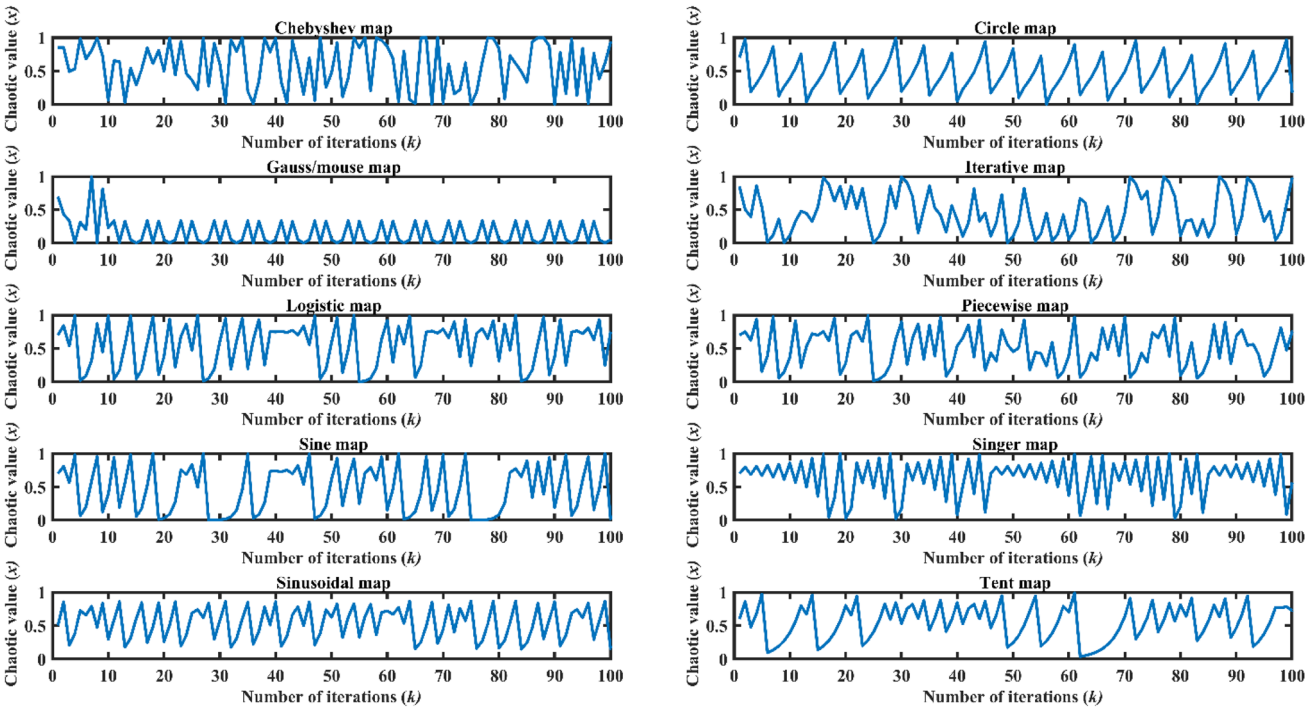

Fig. 1 Visualization of chaotic maps [27]

where $r_2(t)$ is the chaotic variable produced from the chaotic map in the tth iteration and S^a represents the direction vector of ath hummingbird. Equation (13) illustrates that the chaotic maps are permitted to switch between omnidirectional, diagonal, and axial flight modes during foraging strategy.

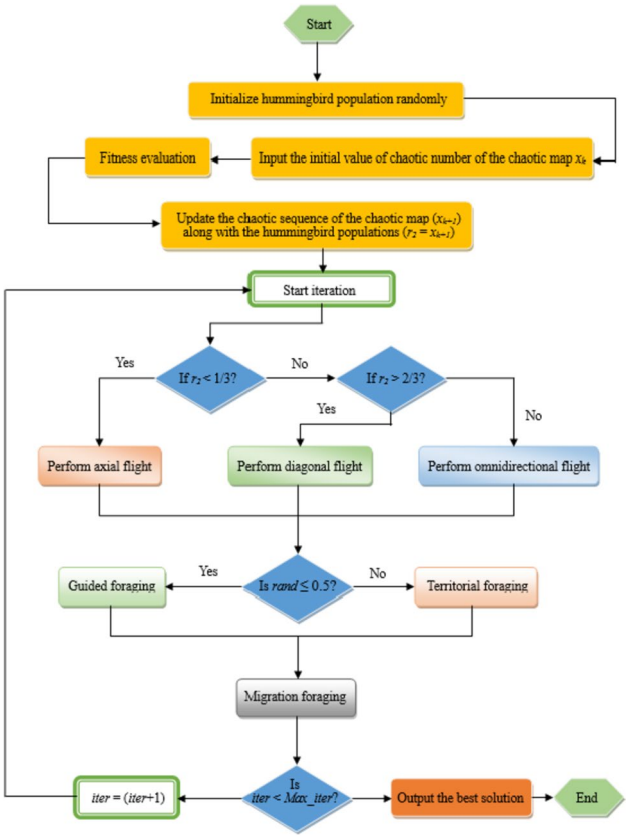

Fig. 2 Flowchart of proposed ChAHA

5 Simulation study on benchmark functions

Whenever a novel optimization algorithm is developed, it must address some pre-defined test functions in order to be examined and evaluated. Performance verification of the proposed meta-heuristic ChAHA method is carried out by implementing extensive simulations on optimization benchmark problems. We have used six widely known unimodal and multimodal benchmark functions to evaluate ChAHA's performance [4]. Unimodal functions are best suited for benchmarking use because they possess single optimum value while multimodal functions are more complicated on account of multiple optima. The term 'global optima' refers to one of the optima, whereas 'local optima' refers to the remaining. Any effective meta-heuristic algorithm should focus on avoiding local optima while discovering the global optimum. Therefore, testing exploration and avoiding being trapped in local optima are the responsibilities of the multimodal benchmark functions. Table 3 lists the characteristics of benchmark unimodal and multimodal functions, with every function having an optimal value of 0 and dimension of 30 while 'Range' denotes the boundary limit of the search space.

5.1 Performance evaluations of ChAHA with different chaotic maps

In order to obtain the outcomes of various ChAHA algorithms, a population size of 50 and 100 iterations are being performed while taking an average across 30 independent

Table 3 Selected benchmark functions employed in present study [4]

No.	Name	Formula	Type	Range
F01	Sphere	$f(x) = \sum_{i=1}^{n} x_i^2$	U, S	[−100,100]
F02	Schwefel 2.22	$f(x) = \sum_{i=1}^{n} \lvert x_i \rvert - \prod_{i=1}^{n} \lvert x_i \rvert$	U, N	[−10,10]
F03	Step	$f(x) = \sum_{i=1}^{n} \left(\lvert x_i \rvert + 0.5 \right)^2$	U, S	[−100,100]
F04	Ackley	$f(x) = -20exp\left(-0.2 \times \sqrt{\frac{1}{n} \sum_{i=1}^{n} x_i^2} \right) - exp\left(\frac{1}{n} \sum_{i=1}^{n} \cos\left(2\pi x_i\right) \right) + 20 + e$	M, N	[−32,32]
F05	Griewank	$f(x) = \frac{1}{4000} \sum_{i=1}^{n} x_i^2 - \prod_{i=1}^{n} \cos\left(\frac{x_i}{\sqrt{i}} \right) + 1$	M, N	[−600,600]
F06	Penalty 1	$f(x) = \frac{\pi}{n} \left\{ 10sin^2\left(\pi y_1\right) + \sum_{i=1}^{n} \left(y_1 - 1\right)^2 \left[1 + 10sin^2\left(\pi y_i + 1\right)\right] + \left(y_n - 1\right)^2 \right\} + \sum_{i=1}^{n} u\left(x_i, 10, 100, 4\right)$ $y_i = 1 + \frac{x_i + 1}{4}$ $u\left(x_i, a, k, m\right) = \begin{cases} k\left(x_i - a\right)^m; & x_i > a \\ 0; & -a < x_i < a \\ k\left(-x_i - a\right)^m; & x_i < -a \end{cases}$	M, N	[−50,50]

Type: *U* unimodal, *S* separable, *M* multimodal, *N* non-separable

runs. As described in Sect. 3, notations ChAHA1 through ChAHA10 employ, respectively, chebyshev, circle, gauss/mouse, iterative, logistic, piecewise, sine, singer, sinusoidal and tent maps. In terms of mean and standard deviation, Table 4 lines up the performance of the original AHA with various ChAHA algorithms for six unimodal and multimodal benchmark functions. The best obtained solutions in Table 4 are emphasised in bold. As seen, ChAHA with tent chaotic map (i.e., ChAHA10) outperforms the traditional AHA and nine chaotic versions of ChAHA in all four metrics in minimizing all the six selected benchmark functions. ChAHA10 achieves the best minimum value which is significantly better than those obtained by other methods for functions F01 to F06. Furthermore, the mean, standard deviation and median values of the considered test functions are notably better (significantly lower values) as computed by ChAHA10. These highlight the effectiveness of ChAHA with tent chaotic map in optimising the objective function through the fact that its results are less scattered and more consistent than those with other nine chaotic map functions, reinforcing its higher and consistent efficacy.

Table 4 Comparison of statistical results of AHA and ten chaotic versions types of ChAHA for six selected benchmark functions

F01 (Sphere)	Mean	Std. Dev.	Median	Best value	F02 (Schwefel 2.22)	Mean	Std. Dev.	Median	Best value
AHA	2.03E+01	1.87E+02	2.50E−12	7.48E−25	AHA	8.47E−01	5.08E+00	7.09E−06	1.67E−13
ChAHA1	4.30E+00	3.61E+01	7.43E−17	4.17E−38	ChAHA1	1.12E−01	6.24E−01	5.14E−09	9.28E−19
ChAHA2	1.20E+01	1.12E+02	5.17E−18	3.19E−37	ChAHA2	3.37E−01	2.27E+00	1.02E−09	1.05E−17
ChAHA3	5.99E+01	5.80E+02	8.79E−16	1.46E−35	ChAHA3	2.68E−01	1.91E+00	1.02E−10	1.52E−19
ChAHA4	2.52E+00	1.29E+01	5.54E−16	1.36E−32	ChAHA4	1.26E−01	3.81E−01	9.84E−10	1.12E−18
ChAHA5	1.59E+01	1.08E+02	1.60E−20	2.99E−38	ChAHA5	3.37E−01	1.92E+00	1.29E−11	9.42E−19
ChAHA6	9.72E+00	7.09E+01	9.33E−20	2.73E−35	ChAHA6	1.85E−01	1.27E+00	5.13E−10	1.44E−17
ChAHA7	1.36E+01	1.10E+02	6.14E−18	4.76E−36	ChAHA7	2.19E−01	1.20E+00	1.63E−09	4.87E−19
ChAHA8	1.90E+00	1.21E+01	4.66E−21	7.38E−35	ChAHA8	1.38E−01	7.52E−01	3.60E−10	6.53E−18
ChAHA9	4.21E+00	2.54E+01	9.19E−19	1.57E−33	ChAHA9	3.74E−01	1.89E+00	4.00E−09	2.74E−19
ChAHA10	**8.70E−01**	**6.63E+00**	**1.14E−25**	**1.49E−41**	ChAHA10	**1.44E−02**	**6.68E−02**	**3.92E−12**	**6.12E−22**
F03 (Step)	Mean	Std. Dev.	Median	Best value	F04 (Ackley)	Mean	Std. Dev.	Median	Best value
AHA	1.11E+02	1.05E+03	4.95E+00	3.17E+00	AHA	2.43E−01	1.77E+00	1.68E−07	8.88E−16
ChAHA1	2.31E+01	1.58E+02	5.24E+00	4.94E+00	ChAHA1	2.79E−01	1.93E+00	3.16E−09	8.88E−16
ChAHA2	2.23E+01	1.02E+02	5.48E+00	5.21E+00	ChAHA2	8.96E−02	5.15E−01	1.47E−10	8.88E−16
ChAHA3	1.59E+01	1.11E+02	4.35E+00	3.50E+00	ChAHA3	1.11E−01	5.86E−01	4.43E−09	8.88E−16
ChAHA4	2.18E+01	1.54E+02	5.64E+00	5.43E+00	ChAHA4	2.55E−01	1.65E+00	4.61E−11	8.88E−16
ChAHA5	6.13E+01	5.13E+02	5.57E+00	5.39E+00	ChAHA5	1.31E−01	6.53E−01	3.23E−10	8.88E−16
ChAHA6	2.39E+01	1.22E+02	5.61E+00	5.22E+00	ChAHA6	1.46E−01	1.02E+00	2.97E−10	8.88E−16
ChAHA7	6.02E+01	4.90E+02	5.23E+00	5.03E+00	ChAHA7	1.06E−01	7.15E−01	1.12E−09	8.88E−16
ChAHA8	1.09E+01	3.79E+01	5.10E+00	4.92E+00	ChAHA8	1.49E−01	8.51E−01	2.52E−10	8.88E−16
ChAHA9	6.80E+01	6.23E+02	4.91E+00	4.71E+00	ChAHA9	1.86E−01	9.81E−01	1.20E−09	8.88E−16
ChAHA10	**4.36E+00**	**4.54E+00**	**3.23E+00**	**2.73E+00**	ChAHA10	**1.29E−02**	**4.24E−02**	**9.52E−12**	**8.88E−16**
F05 (Griewank)	Mean	Std. Dev.	Median	Best value	F06 (Penalty1)	Mean	Std. Dev.	Median	Best value
AHA	2.13E+00	1.66E+01	3.69E−10	0.00E+00	AHA	4.05E+04	4.05E+05	6.73E−01	2.46E−01
ChAHA1	5.31E−01	3.07E+00	0.00E+00	0.00E+00	ChAHA1	9.40E−01	3.87E−01	8.52E−01	7.61E−01
ChAHA2	5.33E−02	2.65E−01	0.00E+00	0.00E+00	ChAHA2	5.50E−01	6.14E−01	3.61E−01	3.20E−01
ChAHA3	9.64E−02	5.28E−01	1.11E−16	0.00E+00	ChAHA3	7.84E−01	1.65E+00	4.97E−01	4.14E−01
ChAHA4	2.41E−01	1.37E+00	1.90E−14	0.00E+00	ChAHA4	1.20E+00	6.62E+00	3.55E−01	2.95E−01
ChAHA5	1.32E−01	5.45E−01	0.00E+00	0.00E+00	ChAHA5	9.20E−01	1.59E+00	5.29E−01	4.40E−01
ChAHA6	2.56E−01	1.59E+00	0.00E+00	0.00E+00	ChAHA6	6.43E−01	5.17E−01	4.53E−01	4.38E−01
ChAHA7	8.55E−02	3.44E−01	0.00E+00	0.00E+00	ChAHA7	6.46E−01	6.91E−01	4.06E−01	3.21E−01
ChAHA8	6.01E−01	5.32E+00	4.77E−15	0.00E+00	ChAHA8	7.72E−01	2.19E+00	3.41E−01	2.94E−01
ChAHA9	3.75E−01	2.62E+00	0.00E+00	0.00E+00	ChAHA9	5.71E−01	4.63E−01	3.91E−01	2.61E−01
ChAHA10	**2.98E−02**	**1.65E−01**	**0.00E+00**	**0.00E+00**	ChAHA10	**3.03E−01**	**2.94E−01**	**2.18E−01**	**1.63E−01**

Bold values indicate the best obtained result

5.2 Statistical testing

Statistical tests should be performed to assess the effectiveness of meta-heuristic algorithms [41]. In particular, it is insufficient to compare algorithms using mean and standard deviation data [42], rather a statistical test needs to be conducted to demonstrate that a proposed novel algorithm significantly outperforms existing algorithms. The 5% significance threshold of the Wilcoxon's rank-sum test [43], a nonparametric statistical test, is employed to determine whether the outcomes of the algorithms differ from each other statistically significantly. For the pair-wise comparison of the best result obtained from all iterations with a 5% significance threshold, Table 5 displays the p-values derived using the Wilcoxon's rank-sum test carried out on the selected benchmark functions. This evaluation is carried out to evaluate if the proposed ChAHA algorithms offer a noticeable improvement over the original ChAHA. As can be seen, majority of the results are less than 0.05, indicating the statistical significance of proposed ChAHA variants. Finally, from Tables 4 and 5, it can be inferred that embedding chaotic map attributes promotes clear avoidance of local optima and the rapid attainment of global optima. This is because using chaotic variables during the ChAHA optimisation process strikes a good balance between exploitation and exploration. We decide that the tent chaotic map is probably the best appropriate map based on all the results that were generated.

5.3 Graphical analysis

The performance of all algorithms was additionally subjected to graphical analysis for more thorough evaluation. The convergence curves of several benchmark functions using the various versions of ChAHA algorithms are shown in Figs. 3, 4, 5, 6, 7 and 8, thereby making it easier to understand the algorithm's rate of convergence. The graphs have been presented on 100 iterations in order to properly observe and analyse the convergence curves of ChAHA on various chaotic maps.

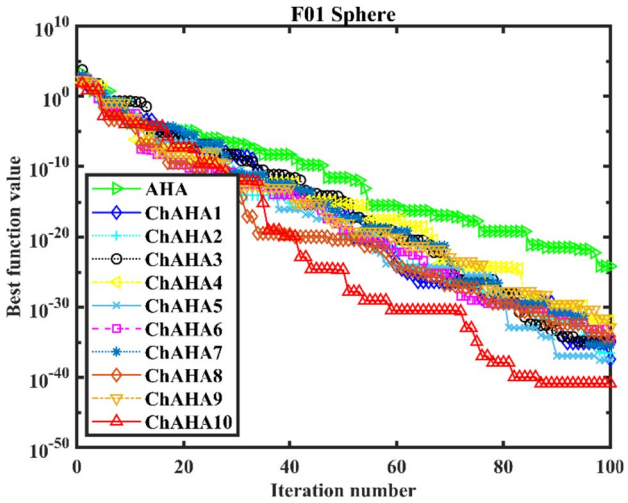

Fig. 3 Performance analysis of proposed ChAHA on the F01 Sphere benchmark function

The values determined by all ten chaotic maps on the F01 Sphere function are shown in Fig. 3. As this function contains a singular global value (i.e., 0), it is simple to solve. As can be seen from the figure, ChAHA with tent chaotic map (i.e., ChAHA10) outperforms all other solutions and has the fastest rate of convergence to the overall solution.

The function values for the F02 Schwefel 2.22 function are shown in Fig. 4. Based on this figure, ChAHA with tent chaotic map (i.e., ChAHA10) beats all other nine methods in this unimodal benchmark function and has an even rate of convergence towards the global solution.

Table 5 Comparison of obtained p-values of the Wilcoxon rank-sum test using AHA and ten different versions of ChAHA over six selected benchmark functions

Pair-wise comparison	F01 (Sphere)	F02 (Schwefel 2.22)	F03 (Step)	F04 (Ackley)	F05 (Griewank)	F06 (Penalty 1)
AHA versus ChAHA1	<0.05	<0.05	<0.05	<0.05	<0.05	<0.05
AHA versus ChAHA2	<0.05	<0.05	<0.05	<0.05	<0.05	<0.05
AHA versus ChAHA3	<0.05	<0.05	0.0538	<0.05	<0.05	<0.05
AHA versus ChAHA4	<0.05	<0.05	<0.05	<0.05	<0.05	0.565
AHA versus ChAHA5	<0.05	<0.05	<0.05	<0.05	<0.05	<0.05
AHA versus ChAHA6	<0.05	<0.05	<0.05	<0.05	<0.05	0.624
AHA versus ChAHA7	<0.05	<0.05	<0.05	<0.05	<0.05	0.508
AHA versus ChAHA8	<0.05	<0.05	<0.05	<0.05	<0.05	<0.05
AHA versus ChAHA9	<0.05	<0.05	<0.05	<0.05	<0.05	<0.05
AHA versus ChAHA10	<0.05	<0.05	<0.05	<0.05	<0.05	<0.05

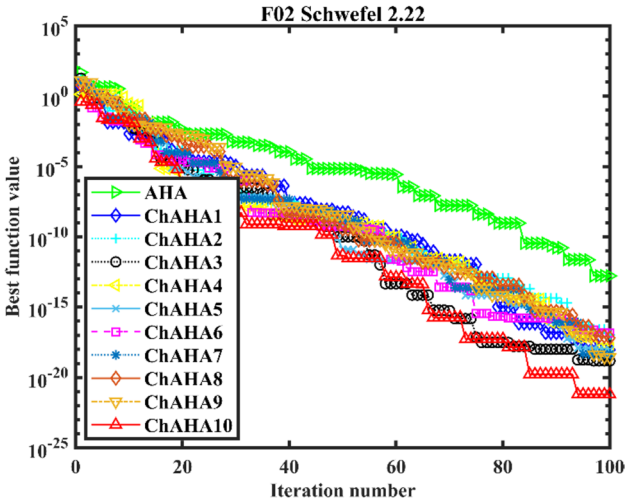

Fig. 4 Performance analysis of proposed ChAHA on the F02 Schwefel 2.22 benchmark function

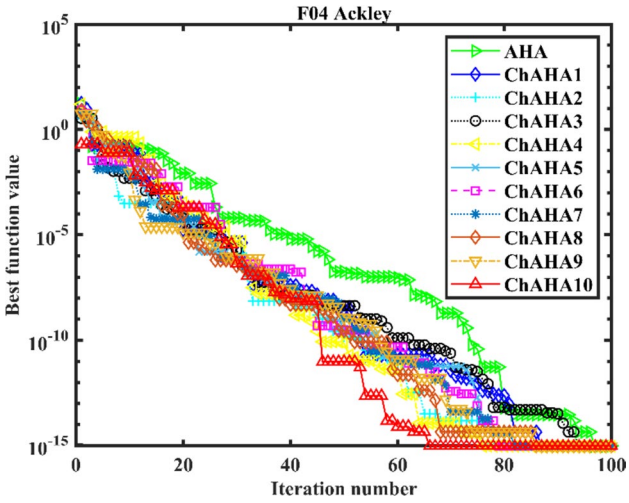

Fig. 6 Performance analysis of proposed ChAHA on the F04 Ackley benchmark function

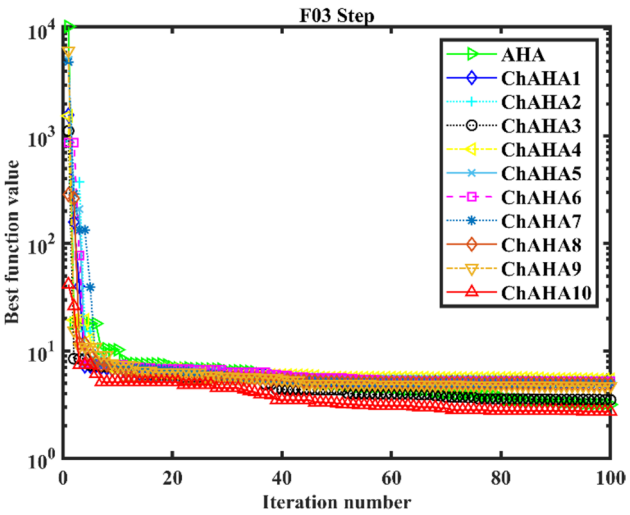

Fig. 5 Performance analysis of proposed ChAHA on the F03 Step benchmark function

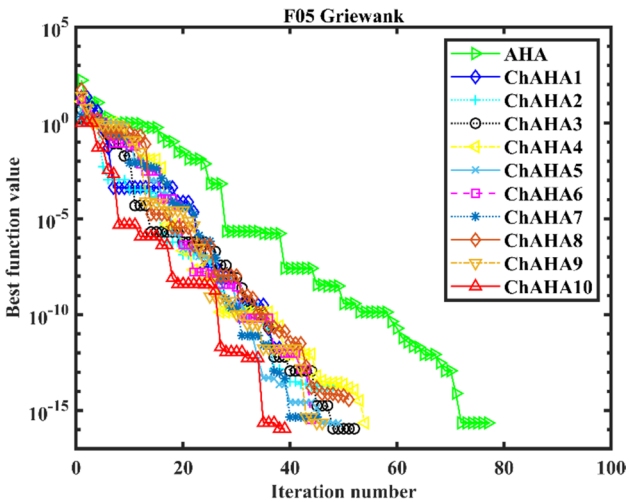

Fig. 7 Performance analysis of proposed ChAHA on the F05 Griewank benchmark function

The function values for the F03 Step function are shown in Fig. 5. As can be observed, even though all chaotic approaches have relatively similar convergence rates, ChAHA with tent chaotic map (i.e., ChAHA10) performs somewhat better in obtaining the optimal solution with gauss chaotic map (i.e., ChAHA3) performing the second best.

Figure 6 shows the values obtained for the ten chaotic techniques employing the F04 Ackley function, a multimodal benchmark function. As can be seen, ChAHA with tent chaotic map (i.e., ChAHA10) excels all other techniques in reaching the global optimum value.

Figure 7 presents the functions values for the F05 Griewank function. It is instantly apparent that the ChAHA with tent map (i.e., ChAHA10) has got the fastest convergence rate since it is able to reach the optimum value in just about 40 iteration numbers, a much smaller value compared to other chaotic approaches.

Figure 8 displays the function values for the F06 Penalty 1 function. It is seen that ChAHA with tent map (i.e., ChAHA10) has the rapid rate of convergence towards the

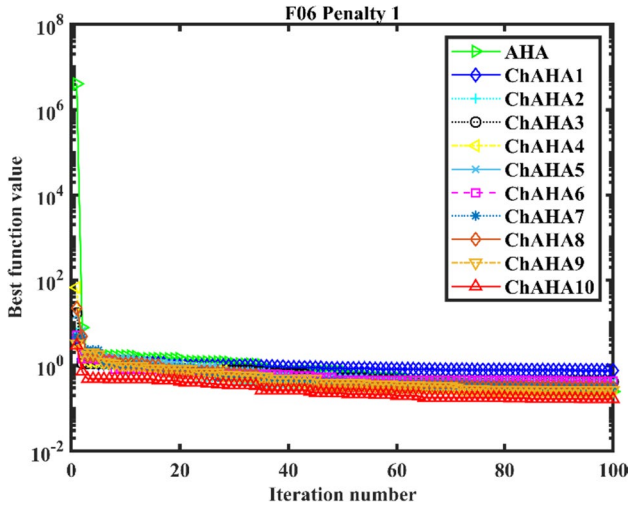

Fig. 8 Performance analysis of proposed ChAHA on the F06 Penalty 1 benchmark function

global solution with sinusoidal chaotic map (i.e., ChAHA9) being the second best.

Finally, it may be concluded from the results presented in Figs. 3, 4, 5, 6, 7 and 8 that ChAHA performs more effectively than AHA. Additionally, ChAHA with tent map (i.e., ChAHA10) has delivered superior outcomes on all the six benchmark functions when compared to other nine chaotic maps. Hence, the authors have selected only ChAHA with tent chaotic map for further investigation on constrained FOPID controller optimization.

6 DC motor with FOPID controller

6.1 Mathematical model of DC motor

In this current work, a separately-excited DC motor has been chosen whose speed needs to be regulated with the use of a FOPID controller. Equivalent circuit of a DC motor (separately-excited) has been represented in Fig. 9 while Fig. 10

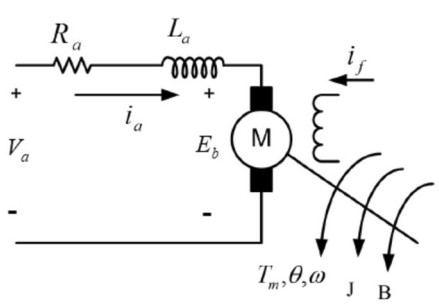

Fig. 9 Equivalent electric circuit of a separately-excited DC motor

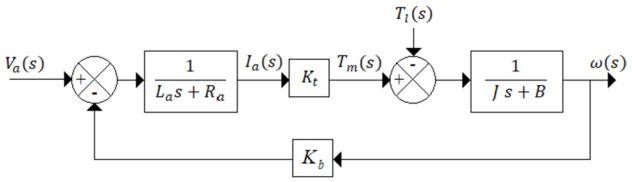

Fig. 10 Block diagram representation of DC motor

shows the block diagram of it. The dynamic characteristics of DC motor in the s-domain can be represented from Eqs. (14) to (19).

$$V_a(s) = \left(R_a + L_a s\right) I_a(s) + E_b(s) \tag{14}$$

$$E_b(s) = K_b \omega(s) \tag{15}$$

$$I_a(s) = \frac{V_a(s) - K_b \omega(s)}{(R_a + L_a s)} \tag{16}$$

$$T_m(s) = K_t I_a(s) \tag{17}$$

$$T_m(s) = K_t \left\{ \frac{V_a(s) - K_b \omega(s)}{(R_a + L_a s)} \right\} \tag{18}$$

$$\omega(s) = \frac{T_m(s) - T_l(s)}{(B + Js)} \tag{19}$$

where V_a denotes terminal voltage in volt, L_a denotes armature inductance in Henry while R_a denotes armature resistance in Ohm, I_a denotes armature current in ampere, E_b denotes back electromotive force (emf) in volt, K_b denotes back emf constant in V s, ω denotes rotor angular velocity in rad/s, T_m denotes motor torque in N m, K_t denotes motor torque constant in N m/A, T_l denotes load torque in N m while, B denotes friction co-efficient in N m s/rad, and J denotes rotor moment of inertia in kg m^2 [44].

Finally, Eq. (20) illustrates the open-loop transfer function under the ideal no-load situation (T_l=0), and can also be used to describe the system plant.

$$G(s)_P = \frac{\omega(s)}{V_a(s)} = \frac{K_t}{\left(L_a s + R_a\right)(Js + B) + K_b K_t} \tag{20}$$

6.2 Mathematical model of FOPID controller

FOPID controller is an advanced variant of the classical PID controller that incorporates a fractional calculus element into its design. It is characterized by certain additional tuning parameters than traditional PID controller which allows

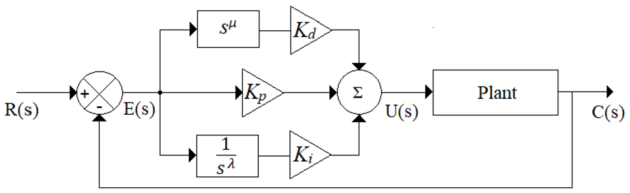

Fig. 11 Basic architecture of FOPID controller

more nuanced and fine-tuned control over the system, particularly in situations where there are complex dynamics or non-linearities. Figure 11 shows the basic architecture of FOPID controller in parallel form. However, the increased complexity of FOPID controller can make it more difficult to design and implement as the fractional order require more complex mathematical calculations [34]. Its transfer function is given in Eq. (21) consisting of the variables K_p, as proportional gain, K_i as integral gain, K_d as derivative gain, λ as fractional integral order term, and μ as fractional derivative order term.

$$G(s)_{FOPID} = K_p + K_i s^{-\lambda} + K_d s^{\mu}, (\lambda, \mu > 0) \tag{21}$$

Table 6 Specifications of chosen DC motor [44]

Motor parameter	Value	Unit
Armature resistance (R_a)	0.4	Ω
Armature inductance (L_a)	2.7	H
Rotor moment of inertia (J)	0.0004	kg m^2
Viscous friction coefficient (B)	0.0022	N m s/rad
Torque constant (K_t)	0.015	N m/A
Back emf constant (K_b)	0.05	V s

$$G_P(s) = \frac{0.015}{0.00108s^2 + 0.0061s + 0.00163} \tag{22}$$

The forward path open loop transfer function as given by Eq. (23) is obtained by the product of transfer functions of controller (FOPID) given by Eq. (21) and plant (DC motor) given by Eq. (22).

$$G_F(s) = \frac{0.015K_d s^{(\mu+\lambda)} + 0.015K_p s^{\lambda} + 0.015K_i}{0.00108s^{(2+\lambda)} + 0.0061s^{(1+\lambda)} + 0.00163s^{\lambda}} \tag{23}$$

Therefore, the transfer function of FOPID controller-based DC motor (closed loop) with unitary feedback ($H(s) = 1$) is determined by Eq. (24).

$$G_{CL}(s)_{FOPID} = \frac{0.015K_d s^{(\mu+\lambda)} + 0.015K_p s^{\lambda} + 0.015K_i}{0.00108s^{(2+\lambda)} + 0.0061s^{(1+\lambda)} + 0.015K_d s^{(\mu+\lambda)} + \left(0.00163 + 0.015K_p\right)s^{\lambda} + 0.015K_i} \tag{24}$$

6.3 Design of a closed loop DC motor system using a FOPID controller

Figure 12 demonstrates a closed loop DC motor system employing a FOPID controller. Here, ω, the measured motor speed, is being compared with ω_{ref}, the reference speed, to calculate the error E, which is then fed as input to the FOPID controller, being represented by its transfer function given by Eq. (21). The controller output U is then fed as input to the DC motor, also represented by its transfer function given by Eq. (20). Table 6 outlines the specifications of the chosen DC motor for this study.

Putting the corresponding DC motor parameters values from Table 6 in Eq. (20), the transfer function of the DC motor (open loop) is given by Eq. (22).

7 Mathematical problem formulation

7.1 Objective function and constraints

The choice of objective or fitness function is crucial because it defines the goal of the optimization process. To perform a fair comparison with [37–39], identical fitness function, Integral of Time multiplied by Absolute Error (ITAE), is considered in this study and is mathematically represented by Eq. (25).

$$ITAE = \int_0^t t \cdot |e(t)| \cdot dt \tag{25}$$

where $e(t)$ stands for time dependent error signal and t denotes the computation time (second).

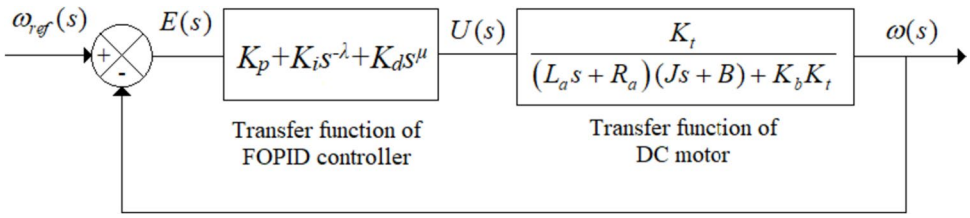

Fig. 12 DC motor speed control system using a FOPID controller (closed loop)

Table 7 Parameter values used for ChAHA

Parameter	Value
Dimension size (m)	5
Population size (N)	50
Maximum iteration number (T)	100
Tent chaotic map paremeter (x_0)	0.27
Lower bound for [K_p; K_i; K_d; λ; μ]	[0.001; 0.001; 0.001; 0; 0]
Upper bound for [K_p; K_i; K_d; λ; μ]	[20; 20; 20; 2; 2]

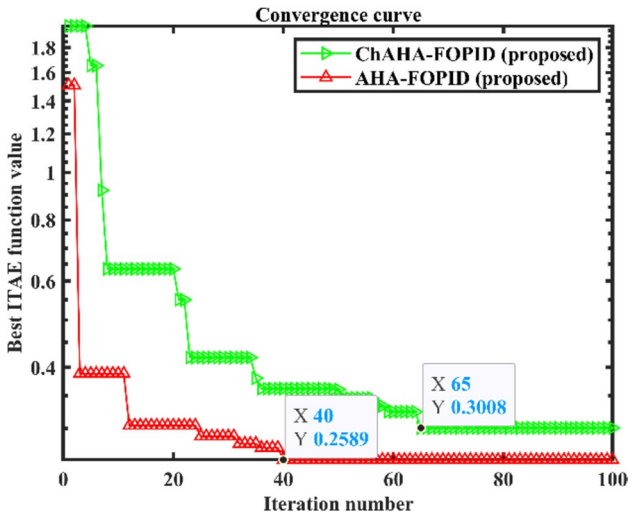

Fig. 13 Convergence curves of ITAE objective function for ChAHA-FOPID and AHA-FOPID controllers

7.2 Implementation of proposed ChAHA-FOPID controller in speed control of DC motor

After designing the proposed ChAHA-FOPID controller, it is implemented for the speed control of DC motor drive system in MATLAB/Simulink (version R2020a) platform through programming codes and its transient response performances are compared with other existing controllers along with robustness analysis by means of a personal computer equipped with a 2.5 GHz based Intel ® i5 processor with a RAM of 8.00 GB. The necessary parameters with their associated values of proposed ChAHA are listed in Table 7.

Table 8 FOPID controller optimum values with different algorithms

Controller genre	Gain parameters				
	K_p	K_i	K_d	λ	μ
ChAHA-FOPID (proposed)	19.8051	19.8679	7.6572	0.334	0.9238
AHA-FOPID (proposed)	19.8934	14.6533	6.6343	0.43	0.9145
GWO-FOPID [37]	18.328	4.9418	3.2612	0.9998	0.9845
ASO-FOPID [38]	19.3282	7.9728	4.7805	0.9755	0.9428
MRFO-FOPID [39]	19.0527	6.3585	5.3293	0.9466	0.9222

Table 9 Comparison of transient reaction analysis for various controllers

Controller genre	Transient reaction standards		
	t_r (s)	t_s (s)	M_p (%)
ChAHA-FOPID (proposed)	**0.0263**	**0.0413**	**0.0000**
AHA-FOPID (proposed)	0.0302	0.0464	0.5996
GWO-FOPID [37]	0.0488	0.0814	0.3145
ASO-FOPID [38]	0.0376	0.0616	**0.0000**
MRFO-FOPID [39]	0.0355	0.0562	0.1546

Bold values indicate the best obtained result

For obtaining the optimal controlling parameter values of FOPID controller in the process of minimization of ITAE fitness function, the convergence curves of AHA and ChAHA are shown in Fig. 13. The best ITAE fitness values estimated by the proposed ChAHA-FOPID controller is found to be 0.2589 at 40th iteration while for AHA-FOPID controller is found to be 0.3008 at 65th iteration.

Following a successful optimization procedure that lasted till maximum number of iterations is reached, the optimal parameters of ChAHA-FOPID and AHA-FOPID controllers so obtained are listed in Table 8. Substituting these optimal controller values in Eq. (24), the transfer functions of ChAHA-FOPID and AHA-FOPID controllers (closed loop) are obtained as given in Eqs. (26) and (27) respectively.

$$G_{CL}(s)_{ChAHA\text{-}FOPID} = \frac{0.1149s^{1.2578} + 0.2971s^{0.334} + 0.298}{0.00108s^{2.334} + 0.0061s^{1.334} + 0.1149s^{1.2578} + 0.2987s^{0.334} + 0.298} \tag{26}$$

$$G_{CL}(s)_{AHA\text{-}FOPID} = \frac{0.0995s^{1.3445} + 0.2984s^{0.43} + 0.2198}{0.00108s^{2.43} + 0.0061s^{1.43} + 0.0995s^{1.3445} + 0.3s^{0.43} + 0.2198} \tag{27}$$

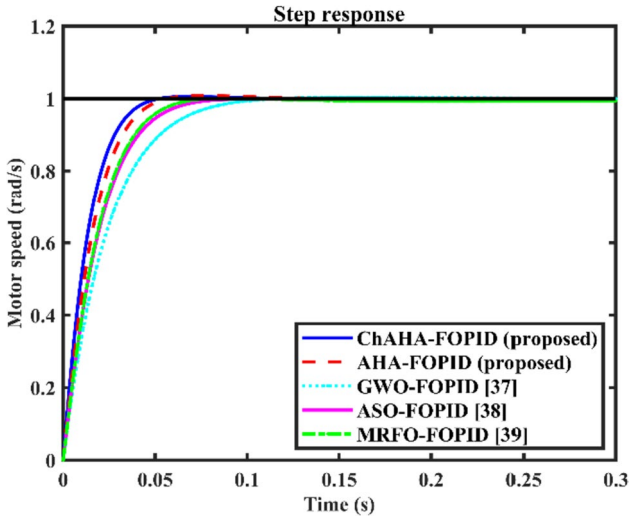

Fig. 14 Comparison of DC motor unit step speed reactions with multiple controllers

Table 10 Different operating cases of DC motor

Motor parameters	Case I	Case II	Case III	Case IV
R_a (in Ω)	0.2	0.2	0.6	0.6
K_t (in Nm/A)	0.0225	0.0075	0.0225	0.0075

8 Comparative analysis

Table 8 lists the FOPID controller optimum values obtained by both proposed and pre-existing algorithms.

Making use of certain renowned optimal standards, such as maximum overshoot (M_p), settling time (t_s) and rise time (t_r), regarding the step response across the time domain norms, Table 9 shows an attempt of performing fair comparative analysis among the proposed and existing state-of-the-art controllers like ChAHA-FOPID (proposed), AHA-FOPID (proposed), GWO-FOPID [37], ASO-FOPID [38], and MRFO-FOPID [39] in regulating the speed of an identical DC motor with the same ITAE objective function. Also, a comparison of unit step speed responses with various controller types is displayed in Fig. 14. From the simulation results, it is quite evident that the proposed ChAHA-FOPID controller exhibits better and improved time response over other existing controllers including AHA-FOPID controller. Hence, the ChAHA-FOPID controller proves its superiority over all other existing controllers with the fastest rise time of 0.0263 s highlighting the ChAHA's higher dynamic reaction in yielding a rapid boost to the target output. In addition, the ChAHA-FOPID controller also possesses the shortest settling time of 0.0413 s, signifying the ChAHA's capability to rapidly stabilize the system's output and efficiently

Table 11 Comparative analysis of transient response among different controller types for Case I

Controller genre	Transient reaction criteria		
	t_r (s)	t_s (s)	M_p (%)
ChAHA-FOPID (proposed)	**0.0183**	**0.0283**	0.8438
AHA-FOPID (proposed)	0.0189	0.0292	0.9054
GWO-FOPID [37]	0.0206	0.0319	0.8845
ASO-FOPID [38]	0.0196	0.0727	4.7876
MRFO-FOPID [39]	0.023	0.0364	**0.6177**

Bold values indicate the best obtained result

Table 12 Comparative analysis of transient response among different controller types for Case II

Controller genre	Transient reaction criteria		
	t_r (s)	t_s (s)	M_p (%)
ChAHA-FOPID (proposed)	**0.0466**	**0.0736**	**0.0000**
AHA-FOPID (proposed)	0.0477	0.075	0.2172
GWO-FOPID [37]	0.0504	0.0795	0.4587
ASO-FOPID [38]	0.0531	0.1701	4.2366
MRFO-FOPID [39]	0.0514	0.0843	0.5024

Bold values indicate the best obtained result

Table 13 Comparative analysis of transient response among different controller types for Case III

Controller genre	Transient reaction criteria		
	t_r (s)	t_s (s)	M_p (%)
ChAHA-FOPID (proposed)	**0.0204**	**0.0319**	0.3172
AHA-FOPID (proposed)	0.0233	0.036	0.4896
GWO-FOPID [37]	0.0279	0.046	**0.2596**
ASO-FOPID [38]	0.0208	0.0831	7.3971
MRFO-FOPID [39]	0.0286	0.0471	0.2798

Bold values indicate the best obtained result

Table 14 Comparative analysis of transient response among different controller types for Case IV

Controller genre	Transient reaction criteria		
	t_r (s)	t_s (s)	M_p (%)
ChAHA-FOPID (proposed)	**0.0507**	**0.0777**	**0.0000**
AHA-FOPID (proposed)	0.0598	0.0932	0.1016
GWO-FOPID [37]	0.066	0.1053	0.2402
ASO-FOPID [38]	0.0531	0.1695	4.1961
MRFO-FOPID [39]	0.0696	0.1108	0.2897

Bold values indicate the best obtained result

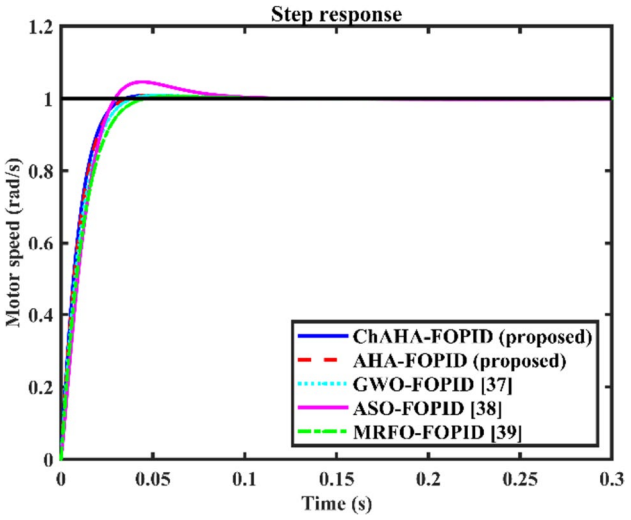

Fig. 15 Output unit step speed reactions of DC motor using different controller types for Case I

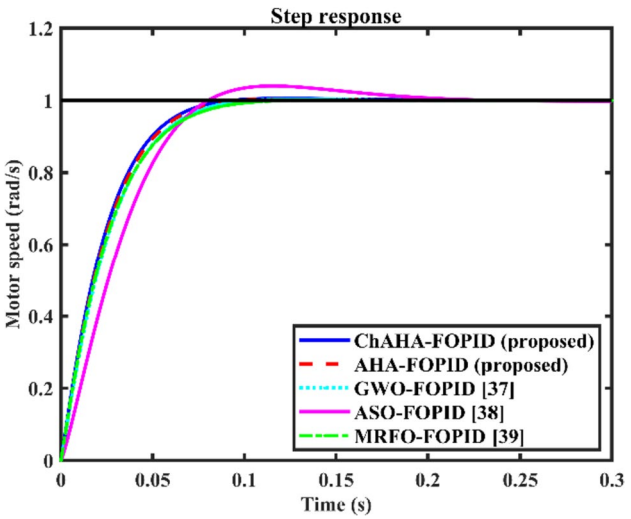

Fig. 16 Output unit step speed reactions of DC motor using different controller types for Case II

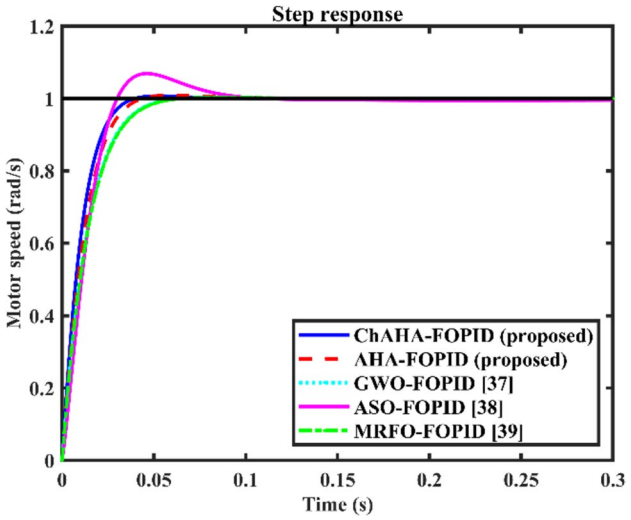

Fig. 17 Output unit step speed reactions of DC motor using different controller types for Case III

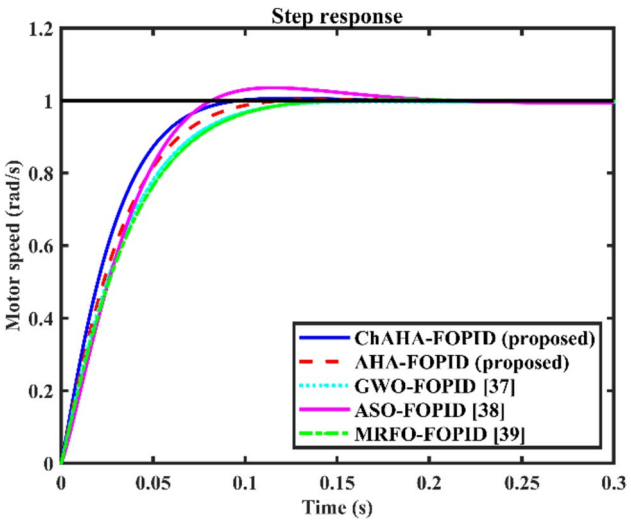

Fig. 18 Output unit step speed reactions of DC motor using different controller types for Case IV

minimize transient oscillations. The aforementioned controller also shows zero overshoot which demonstrates an enhanced and accurate control to the step input without overshooting.

9 Robustness analysis

When a system maintains its stable state in the context of anomalous events, it is considered robust. The proposed system's robustness is examined by monitoring how the system responds to variations in a few motor parameters, such as electrical phase resistance (R_a) of $\pm 50\%$ and torque constant (K_t) of $\pm 50\%$. Following these modifications, a thorough comparative analysis was conducted, resulting in the four potential operating scenarios that are displayed in Table 10.

Tables 11, 12, 13 and 14 present a comparison among simulation results of transient response of speed control with reference to time domain for the selected DC motor using the proposed ChAHA-FOPID and AHA-FOPID controllers as well as existing GWO-FOPID [37], ASO-FOPID [38] and MRFO-FOPID [39] controllers for all the four cases as mentioned in Table 10, while Figs. 15, 16, 17 and 18 show the comparative step response profiles of the DC motor for

each of the respective cases of robust analysis. It can be however referred from these tables and figures that the proposed ChAHA-FOPID controller produces the least settling and rise times accompanied by zero overshoot except in Cases I and III where it exhibits negligible overshoot values as compared to other controllers. Finally, it can be concluded that the proposed ChAHA-FOPID controller delivers a robust performance than the existing controllers under variations in DC motor speed control system parameters.

10 Conclusion and future scope

In this present work, a novel improved meta-heuristic Chaotic Artificial Hummingbird Algorithm (ChAHA) is being proposed by hybridizing chaos theory with Artificial Hummingbird Algorithm (AHA). The key parameter (r_2) of AHA has been controlled through ten distinct chaotic maps. A combination of six different kinds of unimodal and multimodal selective benchmark functions have been utilized to evaluate and confirm ChAHA's performance. The outcomes of the simulation indicate that the original AHA's performance can be greatly improved by the proposed ChAHA, both in terms of exploration and exploitation. Amongst the considered chaotic maps, tent map substantially enhances AHA's performance. The primary factor influencing ChAHA's higher performance is due to chaotic maps creating chaos in the search space which in turn facilitates in finding the optimized solution more rapidly, thereby improving the algorithm's convergence rate. To validate the proposed approach, ChAHA with tent map is employed for efficient tuning of FOPID controller in DC motor speed control. Designing of the FOPID controller has been performed by utilizing the basic AHA and its hybrid chaotic version through reduction of ITAE objective function. These recommended controllers' performances are contrasted with certain existing cutting-edge controllers including the GWO-FOPID, ASO-FOPID and MRFO-FOPID controllers. It has been confirmed from the comparative analysis results that the proposed ChAHA-FOPID controller exhibits the best transient response profile with least amount of settling and rise times in addition to zero overshoot than the other existing controller types. Furthermore, robustness assessment of ChAHA-FOPID controller has been investigated as well with certain variations in the DC motor parameters and it has been found from the simulated results that the proposed ChAHA-FOPID controller is found to be the most effective in suppressing any abnormal shifts that may arise within the system outcome owing to certain uncertainties.

It would be fascinating to use the ChAHA in subsequent future work to address practical engineering issues including enhancing optimization, solving complex problems, and improving system efficiency across diverse engineering applications, fostering innovation and sustainable solutions. Furthermore, comparison of ChAHA with other existing state-of-the-art optimization techniques can be performed in various engineering domains.

Funding The authors did not receive support from any organization for the submitted work.

Data availability All data generated or analyzed during this work are included in this published article.

Declarations

Conflict of interest The authors declare that there is no conflict of interest regarding the publication of this manuscript.

Ethical approval This article does not contain any studies with human participants or animals performed by any of the authors.

References

1. Yang X-S (2008) Introduction to mathematical optimization: from linear programming to metaheuristics. Cambridge International Science Publishing, Cambridge
2. Wolpert DH, Macready WG (1997) No free lunch theorems for optimization. IEEE Trans Evol Comput 1(1):67–82. https://doi.org/10.1109/4235.585893
3. Yang X-S (2010) Engineering optimization: an introduction with metaheuristic applications. Wiley, Cambridge
4. Zhao W, Wang L, Mirjalili S (2022) Artificial hummingbird algorithm: A new bio-inspired optimizer with its engineering applications. Comput Methods Appl Mech Eng 388:1141940. https://doi.org/10.1016/j.cma.2021.114194
5. Shadman Abid M, Apon HJ, Morshed KA, Ahmed A (2022) Optimal planning of multiple renewable energy-integrated distribution system with uncertainties using artificial hummingbird algorithm. IEEE Access 10:40716–40730. https://doi.org/10.1109/ACCESS.2022.3167395
6. Haddad S, Lekouaghet B, Benghanem M, Soukkou A, Rabhi A (2022) Parameter estimation of solar modules operating under outdoor operational conditions using artificial hummingbird algorithm. IEEE Access 10:51299–51314. https://doi.org/10.1109/ACCESS.2022.3174222
7. Alamir N, Kamel S, Megahed TF, Hori M, Abdelkader SM (2022) Developing an artificial hummingbird algorithm for probabilistic energy management of microgrids considering demand response. Front Energy Res 10:905788. https://doi.org/10.3389/fenrg.2022.905788
8. Fathy A (2022) A novel artificial hummingbird algorithm for integrating renewable based biomass distributed generators in radial distribution systems. Appl Energy 323:119605. https://doi.org/10.1016/j.apenergy.2022.119605
9. Wang J, Li Y, Hu G, Yang M (2022) An enhanced artificial hummingbird algorithm and its application in truss topology engineering optimization. Adv Eng Inform 54:101761. https://doi.org/10.1016/j.aei.2022.101761
10. Ramadan A, Kamel S, Hassan MH, Ahmed EM, Hasanien HM (2022) Accurate photovoltaic models based on an

adaptive opposition artificial hummingbird algorithm. Electronics 11(3):318. https://doi.org/10.3390/electronics11030318
11. Ali MAS, FathimathulSalama Abd Elminaam PD (2022) A feature selection based on improved artificial hummingbird algorithm using random opposition-based learning for solving waste classification problem. Mathematics 10(15):2675. https://doi.org/10.3390/math10152675
12. Elaziz MA, Dahou A, El-Sappagh S, Mabrouk A, Gaber MM (2022) AHA-AO: artificial hummingbird algorithm with Aquila optimization for efficient feature selection in medical image classification. Appl Sci 12(19):9710. https://doi.org/10.3390/app12199710
13. Sarhana S, Shaheen A, El-Sehiemy R, Gafar M (2023) Optimal multi-dimension operation in power systems by an improved artificial hummingbird optimizer. Hum Centric Comput Inf Sci 1:3. https://doi.org/10.22967/HCIS.2023.13.013
14. Yildiz BS, Mehta P, Sait SM, Panagant N, Kumar S, Yildiz AR (2022) A new hybrid artificial hummingbird-simulated annealing algorithm to solve constrained mechanical engineering problems. Mater Test 64(7):1043–1050. https://doi.org/10.1515/mt-2022-0123
15. Emam MM, Houssein EH, Tolba MA, Zaky MM, Hamouda Ali M (2023) Application of modified artificial hummingbird algorithm in optimal power flow and generation capacity in power networks considering renewable energy sources. Sci Rep 13(1):21446. https://doi.org/10.1038/s41598-023-48479-6
16. Alhumade H, Houssein EH, Rezk H, Moujdin IA, Al-Shahrani S (2023) Modified artificial hummingbird algorithm-based single-sensor global MPPT for photovoltaic systems. Mathematics 11(4):979. https://doi.org/10.3390/math11040979
17. Zelinka I, Chen G (2010) Motivation for application of evolutionary computation to chaotic systems. In: Evolutionary algorithms and chaotic systems, pp 3–36. https://doi.org/10.1007/978-3-642-10707-8_1
18. Pecora LM, Carroll TL (1990) Synchronization in chaotic systems. Phys Rev Lett 64(8):821. https://doi.org/10.1103/PhysRevLett.64.821
19. Yang D, Li G, Cheng G (2007) On the efficiency of chaos optimization algorithms for global optimization. Chaos Solitons Fractals 34(4):1366–1375. https://doi.org/10.1016/j.chaos.2006.04.057
20. Kohli M, Arora S (2018) Chaotic grey wolf optimization algorithm for constrained optimization problems. J Comput Des Eng 5(4):458–472. https://doi.org/10.1016/j.jcde.2017.02.005
21. Ahmad M, Alam MZ, Umayya Z, Khan S, Ahmad F (2018) An image encryption approach using particle swarm optimization and chaotic map. Int J Inf Technol 10:247–255. https://doi.org/10.1007/s41870-018-0099-y
22. Misaghi M, Yaghoobi M (2019) Improved invasive weed optimization algorithm (IWO) based on chaos theory for optimal design of PID controller. J Comput Des Eng 6(3):284–295. https://doi.org/10.1016/j.jcde.2019.01.001
23. Arora S, Anand P (2019) Chaotic grasshopper optimization algorithm for global optimization. Neural Comput Appl 31:4385–4405. https://doi.org/10.1007/s00521-018-3343-2
24. Sayed GI, Khoriba G, Haggag MH (2018) A novel chaotic salp swarm algorithm for global optimization and feature selection. Appl Intell 48:3462–3481. https://doi.org/10.1007/s10489-018-1158-6
25. Kaur G, Arora S (2018) Chaotic whale optimization algorithm. J Comput Des Eng 5(3):275–284. https://doi.org/10.1016/j.jcde.2017.12.006
26. Arora S, Singh S (2017) An improved butterfly optimization algorithm with chaos. J Intell Fuzzy Syst 32(1):1079–1088. https://doi.org/10.3233/JIFS-16798
27. Saremi S, Mirjalili S, Lewis A (2014) Biogeography-based optimisation with chaos. Neural Comput Appl 25:1077–1097. https://doi.org/10.1007/s00521-014-1597-x
28. Verma AS, Choudhary A, Tiwari S (2023) A novel chaotic archimedes optimization algorithm and its application for efficient selection of regression test cases. Int J Inf Technol 15(2):1055–1068. https://doi.org/10.1007/s41870-022-01031-7
29. Shinde V, Jha R, Mishra DK (2023) Improved Chaotic Sine Cosine Algorithm (ICSCA) for global optima. Int J Inf Technol. https://doi.org/10.1007/s41870-023-01537-8
30. Bansal B, Sahoo A (2022) Chaotic driven gorilla troops optimizer based NMF approach for integrative analysis of multiple source data. Int J Inf Technol 14(7):3437–3448. https://doi.org/10.1007/s41870-022-00928-7
31. Alam A, Muqeem M (2023) An optimal heart disease prediction using chaos game optimization-based recurrent neural model. Int J Inf Technol. https://doi.org/10.1007/s41870-023-01597-w
32. Mirjalili S, Gandomi AH (2017) Chaotic gravitational constants for the gravitational search algorithm. Appl Soft Comput 53:407–419. https://doi.org/10.1016/j.asoc.2017.01.008
33. Kaveh A, Kaveh A (2017) Chaos embedded metaheuristic algorithms. In: Advances in metaheuristic algorithms for optimal design of structures, pp 375–398. https://doi.org/10.1007/978-3-319-46173-1_12
34. Shah P, Agashe S (2016) Review of fractional PID controller. Mechatronics 38:29–41. https://doi.org/10.1016/j.mechatronics.2016.06.005
35. Izci D, Ekinci S (2023) Fractional order controller design via gazelle optimizer for efficient speed regulation of micromotors. e-Prime-Adv Electr Eng Electron Energy 6:100295. https://doi.org/10.1016/j.prime.2023.100295
36. Izci D, Ekinci S, Zeynelgil HL, Hedley J (2021) Fractional order PID design based on novel improved slime mould algorithm. Electr Power Compon Syst 49(9–10):901–918. https://doi.org/10.1080/15325008.2022.2049650
37. Agarwal J, Parmar G, Gupta R, Sikander A (2018) Analysis of grey wolf optimizer based fractional order PID controller in speed control of DC motor. Microsyst Technol 24:4997–5006. https://doi.org/10.1007/s00542-018-3920-4
38. Hekimoğlu B (2019) Optimal tuning of fractional order PID controller for DC motor speed control via chaotic atom search optimization algorithm. IEEE Access 7:38100–38114. https://doi.org/10.1109/ACCESS.2019.2905961
39. Ekinci S, Izci D, Hekimoğlu B (2021) Optimal FOPID speed control of DC motor via opposition-based hybrid manta ray foraging optimization and simulated annealing algorithm. Arab J Sci Eng 46(2):1395–1409. https://doi.org/10.1007/s13369-020-05050-z
40. Tavazoei MS, Haeri M (2007) Comparison of different onedimensional maps as chaotic search pattern in chaos optimization algorithms. Appl Math Comput 187(2):1076–1085. https://doi.org/10.1016/j.amc.2006.09.087
41. Derrac J, García S, Molina D, Herrera F (2011) A practical tutorial on the use of nonparametric statistical tests as a methodology for comparing evolutionary and swarm intelligence algorithms. Swarm Evol Comput 1(1):3–18. https://doi.org/10.1016/j.swevo.2011.02.002
42. García S, Molina D, Lozano M, Herrera F (2009) A study on the use of non-parametric tests for analyzing the evolutionary algorithms' behaviour: a case study on the CEC'2005 special session on real parameter optimization. J Heurist 15:617–644. https://doi.org/10.1007/s10732-008-9080-4
43. Wilcoxon F (1992) Individual comparisons by ranking methods. In: Breakthroughs in statistics: methodology and distribution.

Springer New York, New York, pp 196–202. https://doi.org/10.1007/978-1-4612-4380-9_16
44. Sarma H, Bardalai A (2023) Tuning of PID controller using driving training-based optimization for speed control of DC motor. In: 2023 4th international conference on computing and communication systems (I3CS), pp 1–8. https://doi.org/10.1109/I3CS58314.2023.10127458